Supporting Information

Designing PIM-1 Microfibers with Tunable Morphology and Porosity via Controlling Solvent/Nonsolvent/Polymer Interactions

Siyao Wang, Kaihang Shi, Anurodh Tripathi, Ushno Chakraborty, Gregory N. Parsons* and Saad A. Khan*

Department of Chemical and Biomolecular Engineering, North Carolina State University, Raleigh, NC 27695, United States

*Email: gnp@ncsu.edu, khan@eos.ncsu.edu

1. Characterization of PIM-1 and Bulk Polymer Properties

Proton Nuclear Magnetic Resonance (^{1}H NMR) of the as-synthesized PIM-1 was acquired in $CDCl_3$ with TMS (^{1}H) as internal standard on a Varian Inova 400 MHz spectrometer. Fourier Transform Infrared (FTIR) spectra of ~ 20 mg of PIM-1 powder was recorded on a Nicolet 6700 infrared spectrometer. Spectra were recorded in transmission mode at a resolution of 4 cm^{-1} in the range of 4000 to 500 cm^{-1}. Gel permeation chromatography (GPC) was carried out using a Waters 2695 separations module. A differential refractive index (DRI) detector (Optilab Rex, Wyatt Technology Co.) was attached and used for molecular weight analysis. The setup had 3 columns in series (Mn ranges: 5−600, 0.05− 100 and 0.5−30 kDa), and the mobile phase was THF with a flow rate of 0.5 mL/min. The columns and detectors were maintained at 25 °C. Conventional calibration was done using six poly (methyl methacrylate) (PMMA) standards from Sigma-Aldrich ranging from 1 to 211 kDa. Thermogravimetric analysis of PIM-1 powder was conducted using a TGA-DTA (SETARAM Setsys Evolution). The temperature gradient consisted of a 10 °C/min ramp to 110 °C, a 1 h hold at 110 °C drying step to remove any adsorbed species, and a 10 °C/min ramp to 1000 °C. The flowrate was maintained at 100 mL/min using He gas.

The structure and purity of the polymer are confirmed by ^{1}H-NMR and FTIR spectra (**Figure S1a-b**). Thermogravimetric analysis of the PIM-1 powder shows that decomposition occurs at 479 °C (**Figure S1c**). The as-synthesized PIM-1 polymer is a fluorescent yellow powder (**Figure S1e**) with a molecular weight (Mw) of ~100 kDa and a PDI of 1.98. The molecular weight distribution is shown in **Figure S1d**.

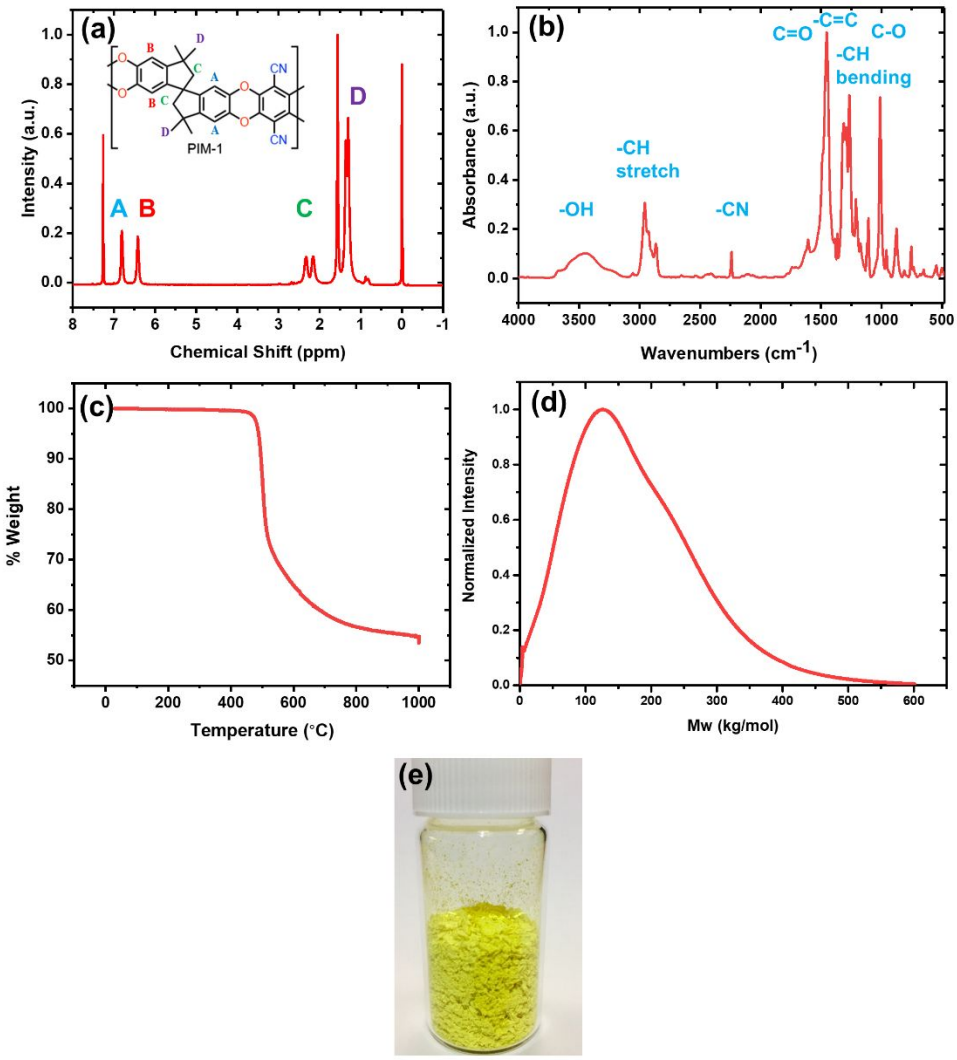

Figure S1. (a) Proton Nuclear Magnetic Resonance (^{1}H NMR) Spectroscopy, (b) Fourier Transform Infrared Spectroscopy (FTIR), (c) TGA (Thermal Gravimetric Analysis) curve, (d) molecular weight distribution of as-synthesized PIM-1, and (e) an optical image of PIM-1 powder.

2. Low Magnification SEM Images of PIM-1 Fibers

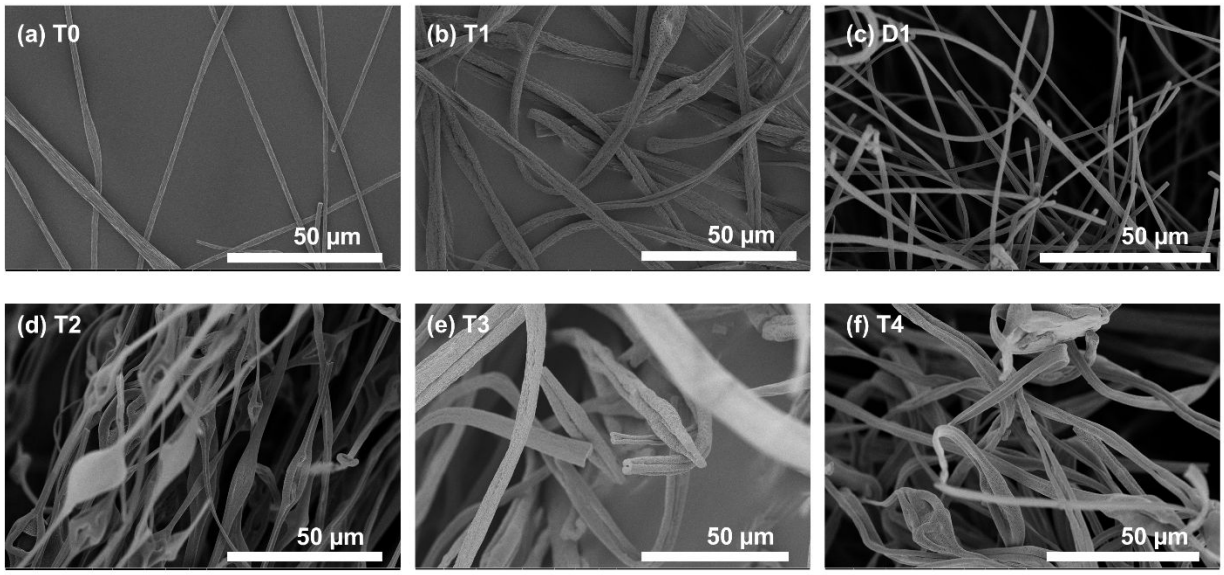

Figure S2. Low magnification SEM images of as-fabricated PIM-1 fibers: (a-c) uniform fiber structure; (d-f) bead-on-string morphology due to low dielectric constant of toluene.

3. Cloud Point Measurement

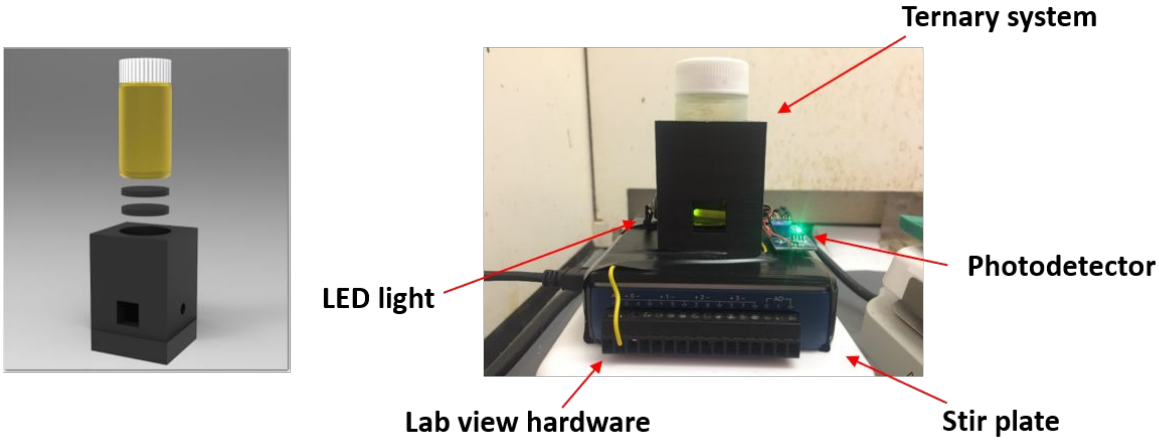

Figure S3. Experimental set up for cloud point measurements.

4. Surface Area and CO_2 Adsorption of PIM Powder and Fiber Samples.

Pore size distribution (**Figure S4b**) of PIM-1 powder was obtained from a smooth-shift nonlocal density functional theory (SSNLDFT) model, which was recently reported to be the most

accurate method for PSD characterization of microporous amorphous materials.[1] From the PSD of PIM-1 powder, a broad distribution of pore size ranging from 0-15 Å is observed, which indicates the large portion of microporosity in this material. The Brunauer-Emmett-Teller (BET) surface area calculated from N_2 adsorption isotherm (**Figure S4a**) is around 750 m^2/g. The maximum pore volume determined at P/P0 = 0.95 of the adsorption isotherm is 0.50 cm^3/g. Pore size distribution of PIM-1 fibers (**Figure S4c-d**) indicates that PIM-1 fiber samples maintain the microporosity from PIM-1 powder.

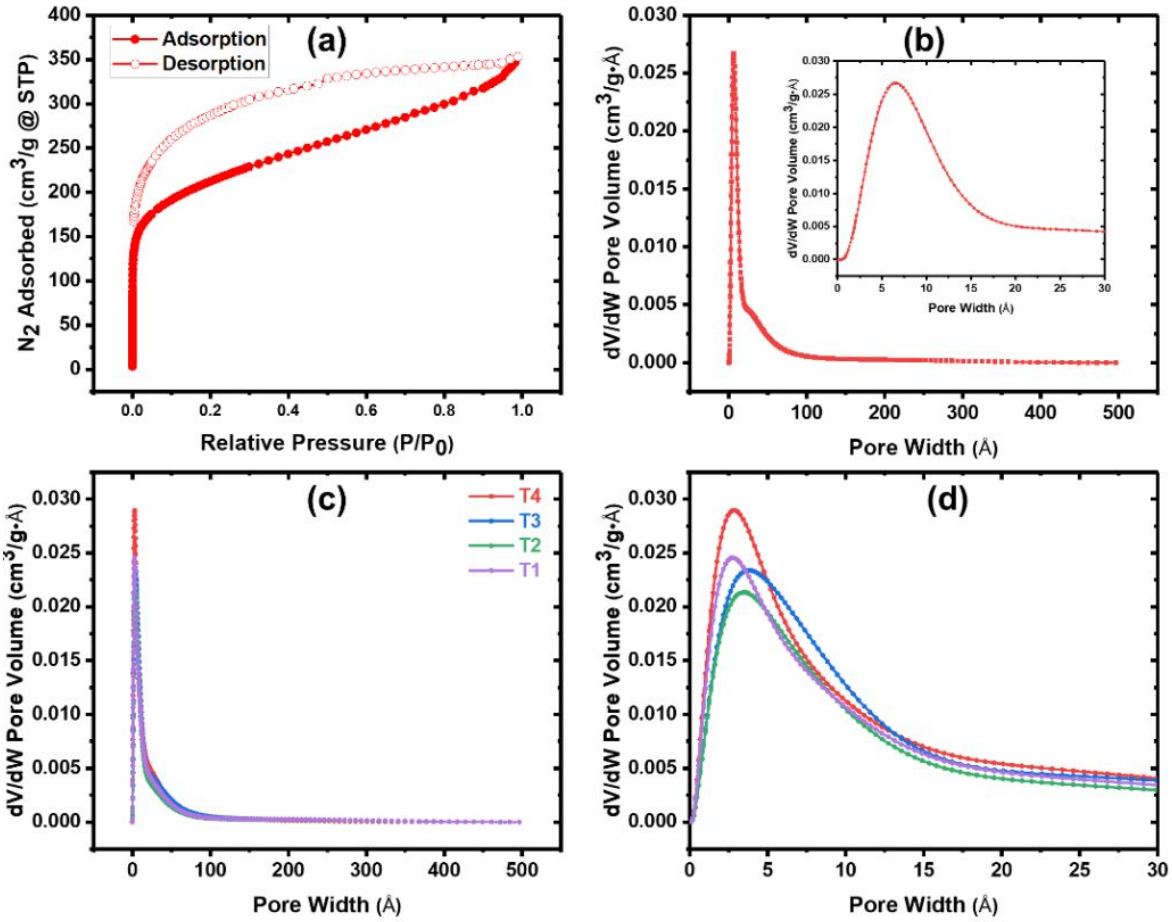

Figure S4. (a) Nitrogen adsorption/desorption isotherms of PIM-1 powder at 77 K and (b) pore size distribution (PSD) via a smooth-shift nonlocal density functional theory (SSNLDFT) model. (c-d) Pore size distribution (PSD) of T1, T2, T3 and T4 fibers via a smooth-shift nonlocal density functional theory (SSNLDFT) model.

Table S1. Surface Area, Pore Volume and Quantity of Adsorbed CO_2 of PIM Powder and Different Fiber Samples.

	PIM-1 powder	T0 fiber	D1 fiber	T1 fiber	T2 fiber	T3 fiber	T4 fiber
Surface Area (m^2/g)	750	660	660	660	605	705	745
Total Pore Volume (cm^3/g)	0.50	0.42	0.40	0.42	0.38	0.45	0.45
CO_2 Adsorbed @273K,1 bar (mmol/g)	2.54	2.03	2.15	2.14	2.03	2.54	2.37

5. Kinetics of CO_2 Adsorption under Different Temperatures.

The kinetic data were fitted to the linear driving force model,[2]

$$\frac{\partial q}{\partial t} = k\left(q_e - q\right) \tag{1}$$

and to the quadratic driving force model,[3]

$$\frac{\partial q}{\partial t} = k\left(q_e - q\right)^2 \tag{2}$$

where q is the adsorbed amount as a function of time t, q_e is the equilibrium adsorbed amount and k is the total mass transfer coefficient. Eq. (1) and Eq. (2) are both first-order differential equations and can be solved exactly. The Eq. (1) leads to a pseudo-first order kinetic model,

$$q = q_e - q_e e^{-kt} \tag{3}$$

and the Eq. (2) leads to a pseudo-second order kinetic model,

$$q = \frac{q_e{}^2 kt}{1 + q_e kt} \tag{4}$$

Eq. (3) and Eq.(4) were fitted directly to the experimental data and the fitted parameters k and q_e are listed in Table S2 and Table S3 for the pseudo-first order and pseudo-second order model, respectively. We can also use the Arrehenius equation to obtain the adsorption activation energy under the operational condition,

$$k = A\exp\left(-\frac{E_a}{RT}\right) \tag{5}$$

Where A is the pre-factor; E_a is the adsorption activation energy and R is the gas constant. To get E_a, we plotted ln$k$ versus $1/T$ and fit the discrete data to a linear function whose slope is $-E_a/R$.

Table S2. Linear driving force mass transfer coefficient at different temperatures and the corresponding adsorption capacity.

Temperature (°C)	k (1/min)	q_e (mmol/g)
25	0.2571	0.1888
50	0.2504	0.08089
75	0.2471	0.03824

Table S3. Quadratic driving force mass transfer coefficient at different temperatures and the corresponding adsorption capacity.

Temperature (°C)	k (1/min)	q_e (mmol/g)
25	1.502	0.2175
50	3.404	0.09348
75	7.021	0.04432

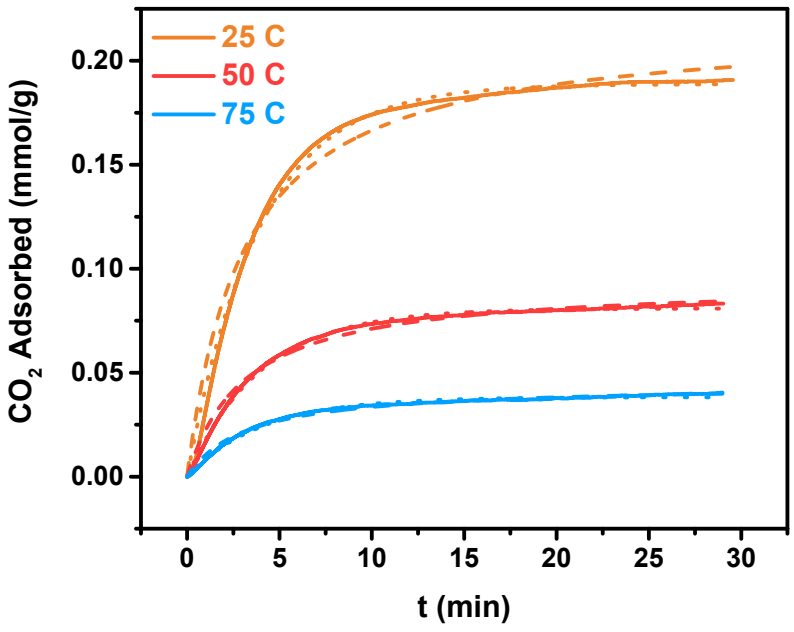

Figure S5. Kinetics of CO_2 adsorption under 25 °C, 50 °C and 75 °C. Solid line: experimental data; dotted line: fitted data using linear driving force model; dashed line: fitted data using quadratic driving force model.

6. Ternary Phase Diagram Calculation Details

The ternary phase diagram of nonsolvent (1)/solvent (2)/polymer (3) is calculated by Flory-Huggins model, and the Gibbs free energy of mixing can be written as

$$\frac{\Delta G_m}{RT} = n_1 \ln \phi_1 + n_2 \ln \phi_2 + n_3 \ln \phi_3 + n_1 \phi_2 g_{12}\left(u_2\right) + n_2 \phi_3 \chi_{23}\left(\phi_3\right) + n_1 \phi_3 \chi_{13} \tag{6}$$

where R is the gas constant and T is temperature; n_i is the number of moles of component *i*; ϕ_i is volume fraction of component *i*; $u_2 = \phi_2 / \left(\phi_1 + \phi_2\right)$ is pseudo binary composition; g_{12}, χ_{23} and χ_{13} are the interaction parameters for nonsolvent-solvent, solvent-polymer and nonsolvent-polymer pairs, respectively, among which we only take g_{12} to be the concentration-dependent variable, while other two interaction parameters, χ_{23} and χ_{13}, are treated as constants. When phases are in thermodynamic equilibrium, we have

$$\Delta\mu_{i,c} = \Delta\mu_{i,d} \quad (i = 1, 2, 3) \tag{7}$$

where $\Delta\mu_{i,c} = \partial\left(\Delta G_m\right) / \partial n_i$ is the chemical potential change of component *i* in the polymer concentrated phase, and the subscript *c* and *d* denotes polymer-concentrated phase and polymer-dilute phase, respectively. From Eq. (6), the chemical potential change for each component can be written as[4]

$$\begin{aligned} \frac{\Delta\mu_1}{RT} = {} & \ln \phi_1 + 1 - \phi_1 - s\phi_2 - r\phi_3 + \left(g_{12}\phi_2 + \chi_{13}\phi_3\right)\left(\phi_2 + \phi_3\right) \\ & - s\phi_2\phi_3\chi_{23} - \phi_2 u_1 u_2 \left(dg_{12} / du_2\right) \end{aligned} \tag{8}$$

$$\frac{s\Delta\mu_2}{RT} = s\ln\phi_2 + s - s\phi_2 - \phi_1 - r\phi_3 + \left(g_{12}\phi_1 + s\chi_{23}\phi_3\right)\left(\phi_1 + \phi_3\right) - \phi_1\phi_3\chi_{13} + \phi_1 u_1 u_2 \left(dg_{12}/du_2\right) \tag{9}$$

$$\frac{r\Delta\mu_3}{RT} = r\ln\phi_3 + r - r\phi_3 - \phi_1 - s\phi_2 + \left(\chi_{13}\phi_1 + s\chi_{23}\phi_2\right)\left(\phi_1 + \phi_2\right) - \phi_1\phi_2 g_{12} \tag{10}$$

where $s = v_1/v_2$ and $r = v_1/v_3$; v_i is the molar volume of component *i*. The nonsolvent-solvent interaction parameter g_{12} is calculated by UNIFAC method[5] using the vapor-liquid equilibrium (VLE) database[6], from which we can obtain the activity coefficient γ_i of each component in the binary mixture. The molar excess Gibbs free energy can be calculated by

$$\frac{\Delta\bar{G}^E}{RT} = x_1\ln\gamma_1 + x_2\ln\gamma_2 \tag{11}$$

where x_i is the mole fraction of component *i* in the binary mixture. If we further assume the Flory-Huggins theory can be applied to nonsolvent-solvent system[7], g_{12} at different ϕ_2 is given by

$$g_{12} = \frac{1}{x_1\phi_2}\left[x_1\ln\left(\frac{x_1}{\phi_1}\right) + x_2\ln\left(\frac{x_2}{\phi_2}\right) + \frac{\Delta\bar{G}^E}{RT}\right] \tag{12}$$

Now we fit the value of g_{12} to a polynomial to the second order and to the fourth order for the Toluene/THF system and DMF/THF system, respectively, as

$$g_{12}\left(\phi_2\right) = -0.00392157\phi_2^2 + 0.0645838\phi_2 + 0.325987 \quad \text{(Toluene/THF)} \tag{13}$$

$$g_{12}\left(\phi_2\right) = 0.5777\phi_2^4 - 0.5866\phi_2^3 + 0.4738\phi_2^2 + 0.2363\phi_2 + 0.5821 \quad \text{(DMF/THF)} \tag{14}$$

To apply Eqs. (13) and (14) to a ternary system, we simply replace ϕ_2 with pseudo binary composition u_2. The solvent-polymer interaction parameter χ_{23} was roughly estimated by[8]

$$\chi_{23} = \chi_s + \chi_h$$
$$= 0.34 + \frac{v_2\left(\delta_2 - \delta_3\right)^2}{RT} \quad (15)$$

where χ_s and χ_h are entropic and enthalpic component, respectively; the entropic contribution is usually chosen to be 0.34 for polymer-solvent system as a rule of thumb[9]; δ_i is the Hildebrand solubility parameter of component i ($\delta_{THF} = 18.5$ $(J/cm^3)^{1/2}$, $\delta_{PIM1} = 19.5$ $(J/cm^3)^{1/2}$), thus the value is $\chi_{23} = 0.3725$. The nonsolvent-polymer interaction parameter χ_{13} is usually obtained from water sorption experiment; however, no experimental data are available for PIM-1 system. Therefore, we here treat χ_{13} as a fitting parameter. When taking $\chi_{13} = 0.7$ for Toluene/PIM-1 pair and $\chi_{13} = 1.7$ for DMF/PIM-1 pair we can get the best agreement with the experimental data. All required parameters in the model are listed in Table 1.

Table S4. Parameters Required by Flory-Huggins Theory to Plot the Ternary Phase Diagram.

System	v_1 (cm^3/mol)	v_2 (cm^3/mol)	v_3 (cm^3/mol)	χ_{13}	χ_{23}
Toluene(1)/THF(2)/PIM-1(3)	106.3	79.76	100,000[a]	0.7	0.3725
DMF(1)/THF(2)/PIM-1(3)	82.6			1.7	

[a] The bulk density of PIM-1 is assumed to be 0.93 g/cm^3[10]

The equilibrium volume fraction of each component in both polymer-concentrated phase and polymer-dilute phase can be solved by minimizing the objective function[4,11],

$$F = \sum_{i=1}^{3} f_i^2 \quad (16)$$

where

$$f_1 = \left(\Delta\mu_{1,c} - \Delta\mu_{1,d}\right)/RT \tag{17}$$

$$f_2 = s\left(\Delta\mu_{2,c} - \Delta\mu_{2,d}\right)/RT \tag{18}$$

$$f_3 = r\left(\Delta\mu_{3,c} - \Delta\mu_{3,d}\right)/RT \tag{19}$$

We used "*fmincon"* function in the MATLAB software to find the minimum of the objective function [Eq. (16)] under constraints, i.e., $\phi_1 + \phi_2 + \phi_3 = 1$, in both polymer-concentrated and polymer-dilute phases. We chose volume fraction of PIM-1 in its dilute phase as the independent variable and solved the other five variables. The spinodal curve can be obtained by solving[4]

$$G_{22}G_{33} - \left(G_{23}\right)^2 = 0 \tag{20}$$

where

$$G_{ij} = \frac{\partial^2 \Delta\overline{G}_M}{\partial\phi_i \partial\phi_j} v_{ref} \tag{21}$$

where $\Delta\overline{G}_M$ is the Gibbs free energy of mixing on a unit-volume basis; v_{ref} is the molar volume of the reference component, which we take to be nonsolvent (component 1). The numerical procedure to solve the spinodal curve [Eq. (20)] is similar to that for the binodal curve; the volume fraction of PIM-1, ϕ_3, was viewed as an independent variable, but "*fsolve"* function was used instead in the MATLAB software to solve Eq. (20). Together with material balance, $\phi_1 + \phi_2 + \phi_3 = 1$, a series of points on the spinodal curve can be obtained at different trial ϕ_3 values. The critical point for the ternary system is governed by[4]

$$G_{222}\left(G_{33}\right)^2 - 3G_{223}G_{23}G_{33} + 3G_{233}\left(G_{23}\right)^2 - G_{22}G_{23}G_{333} = 0 \tag{22}$$

where

$$G_{22} = \frac{1}{\phi_1} + \left(\frac{v_1}{v_2}\right)\frac{1}{\phi_2} - 2g_{12} + 2\left(1-2u_2\right)\left(\frac{dg_{12}}{du_2}\right) + u_1u_2\left(\frac{d^2g_{12}}{du_2{}^2}\right) \tag{23}$$

$$G_{23} = \frac{1}{\phi_1} - \left(g_{12} + \chi_{13}\right) + \left(\frac{v_1}{v_2}\right)\chi_{23} + u_2\left(1-3u_2\right)\left(\frac{dg_{12}}{du_2}\right) + u_1u_2{}^2\left(\frac{d^2g_{12}}{du_2{}^2}\right) \tag{24}$$

$$G_{33} = \frac{1}{\phi_1} + \left(\frac{v_1}{v_3}\right)\frac{1}{\phi_3} - 2\chi_{13} - 2u_2{}^3\left(\frac{dg_{12}}{du_2}\right) + u_1u_2{}^3\left(\frac{d^2g_{12}}{du_2{}^2}\right) \tag{25}$$

$$G_{222} = \frac{1}{\phi_1{}^2} - \left(\frac{v_1}{v_2}\right)\frac{1}{\phi_2{}^2} - 6\frac{u_2}{\phi_2}\left(\frac{dg_{12}}{du_2}\right) + 3\left(1-2u_2\right)\frac{u_2}{\phi_2}\left(\frac{d^2g_{12}}{du_2{}^2}\right) + u_1\frac{u_2{}^2}{\phi_2}\left(\frac{d^3g_{12}}{du_2{}^3}\right) \tag{26}$$

$$G_{223} = \frac{1}{\phi_1{}^2} - 6\frac{u_2{}^2}{\phi_2}\left(\frac{dg_{12}}{du_2}\right) + 3\left(1-2u_2\right)\frac{u_2{}^2}{\phi_2}\left(\frac{d^2g_{12}}{du_2{}^2}\right) + u_1\frac{u_2{}^3}{\phi_2}\left(\frac{d^3g_{12}}{du_2{}^3}\right) \tag{27}$$

$$G_{233} = \frac{1}{\phi_1{}^2} - 6\frac{u_2{}^3}{\phi_2}\left(\frac{dg_{12}}{du_2}\right) + 3\left(1-2u_2\right)\frac{u_2{}^3}{\phi_2}\left(\frac{d^2g_{12}}{du_2{}^2}\right) + u_1\frac{u_2{}^4}{\phi_2}\left(\frac{d^3g_{12}}{du_2{}^3}\right) \tag{28}$$

$$G_{333} = \frac{1}{\phi_1{}^2} - \left(\frac{v_1}{v_3}\right)\frac{1}{\phi_3{}^2} - 6\frac{u_2{}^4}{\phi_2}\left(\frac{dg_{12}}{du_2}\right) + 3\left(1-2u_2\right)\frac{u_2{}^4}{\phi_2}\left(\frac{d^2g_{12}}{du_2{}^2}\right) + u_1\frac{u_2{}^5}{\phi_2}\left(\frac{d^3g_{12}}{du_2{}^3}\right) \tag{29}$$

References:

1. Kupgan, G., Liyana-Arachchi, T. P. & Colina, C. M. NLDFT Pore Size Distribution in Amorphous Microporous Materials. *Langmuir* **33**, 11138–11145 (2017).
2. Landaverde-Alvarado, C., Morris, A. J. & Martin, S. M. Gas sorption and kinetics of CO2 sorption and transport in a polymorphic microporous MOF with open Zn (II) coordination sites. *J. CO2 Util.* **19**, 40–48 (2017).
3. Ho, Y. . & McKay, G. Pseudo-second order model for sorption processes. *Process Biochem.* **34**, 451–465 (1999).
4. Yilmaz, L. & McHugh, A. J. Analysis of nonsolvent–solvent–polymer phase diagrams and their relevance to membrane formation modeling. *J. Appl. Polym. Sci.* **31**, 997–1018 (1986).
5. Fredenslund, A., Jones, R. L. & Prausnitz, J. M. Group-contribution estimation of activity coefficients in nonideal liquid mixtures. *AIChE J.* **21**, 1086–1099 (1975).
6. Gmehling, J., Rasmussen, P. & Fredenslund, A. Vapor-liquid equilibriums by UNIFAC group contribution. Revision and extension. 2. *Ind. Eng. Chem. Process Des. Dev.* **21**, 118–127 (1982).
7. Pouchlý, J. & Živný, A. Correlation of data on preferential sorption using the modified flory-huggins equation. *Die Makromol. Chemie* **183**, 3019–3040 (1982).
8. Pai, C., Boyce, M. C. & Rutledge, G. C. Morphology of Porous and Wrinkled Fibers of Polystyrene Electrospun from Dimethylformamide. *Macromolecules* **42**, 2102–2114 (2009).
9. Brandrup, J., Immergut, E. H. & Grulke, E. A. *Polymer Handbook*. (New York: Wiley-Interscience, c1999., 1999).
10. Frentrup, H., Hart, K., Colina, C. & Müller, E. In Silico Determination of Gas Permeabilities by Non-Equilibrium Molecular Dynamics: CO2 and He through PIM-1. *Membranes (Basel).* **5**, 99–119 (2015).
11. Altena, F. W. & Smolders, C. A. Calculation of liquid-liquid phase separation in a ternary system of a polymer in a mixture of a solvent and a nonsolvent. *Macromolecules* **15**, 1491–1497 (1982).